Electronic Supplementary Information

Guiding Lithium Deposition in Tent-like Nitrogen-doped Porous Carbon Microcavities for Stable Lithium Metal Anodes

He Gan[a], Jing Wu[a], Hui Chen[a, b], Run Li[a, b] *, Hongbo Liu[a, b] *

[a] College of Material Science and Engineering, Hunan University, Changsha, Hunan, 410082, China

[b] Hunan Province Key Laboratory for Advanced Carbon Materials and Applied Technology, Hunan University, Changsha, Hunan, 410082, China

Email: lirun@hnu.edu.cn; hndxlhb@163.com

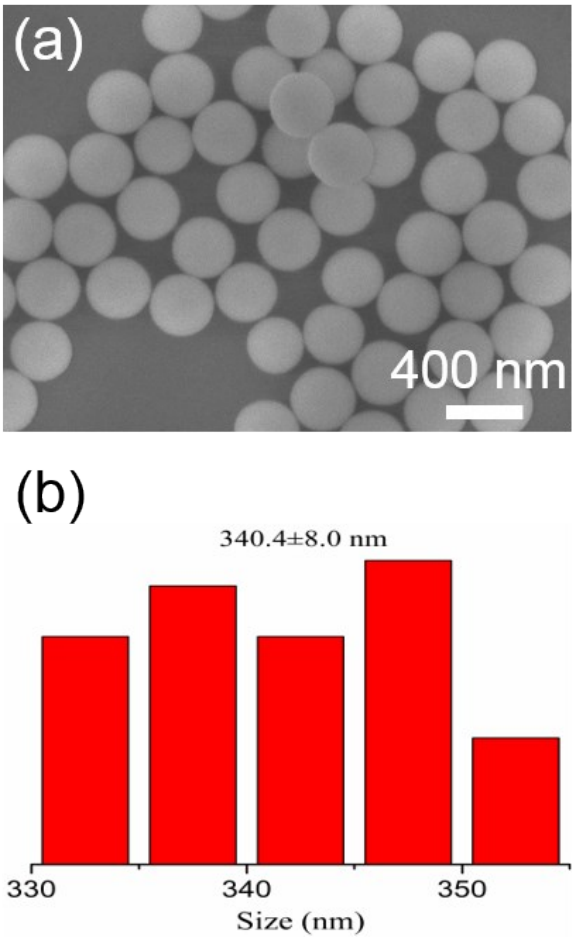

Fig. S1 Monodisperse SiO_2 microspheres prepared by modified Stöber method. SEM image of SiO_2 (a) and corresponding size distribution (b).

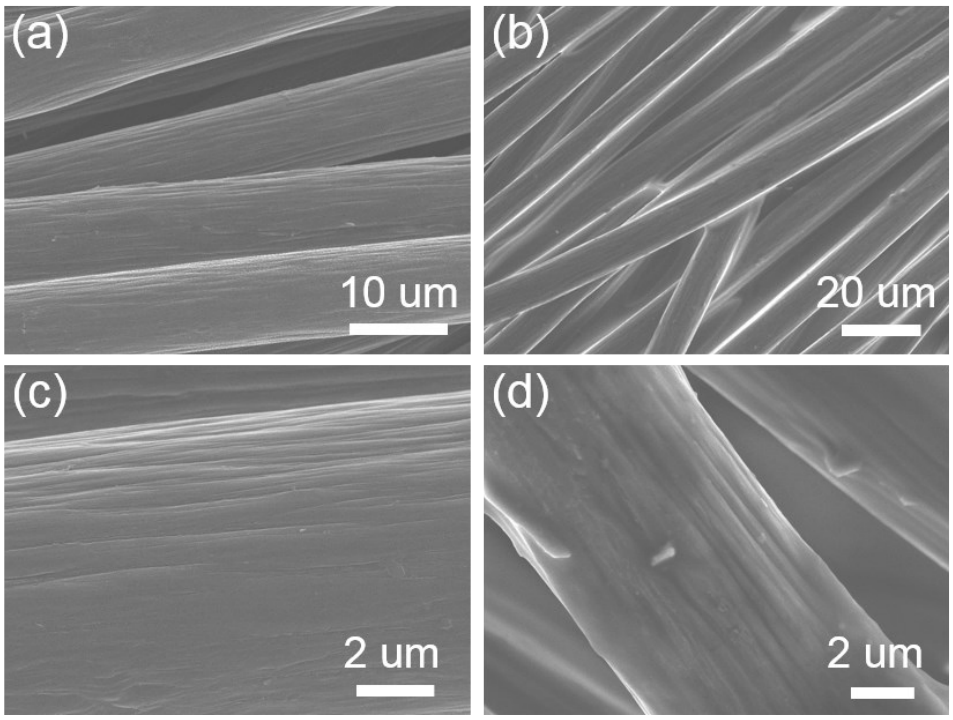

Fig.S2 SEM images of CC (a), (c) and NPC@CC (b), (d). (c) and (d) are magnified SEM images of CC and NPC@CC, respectively.

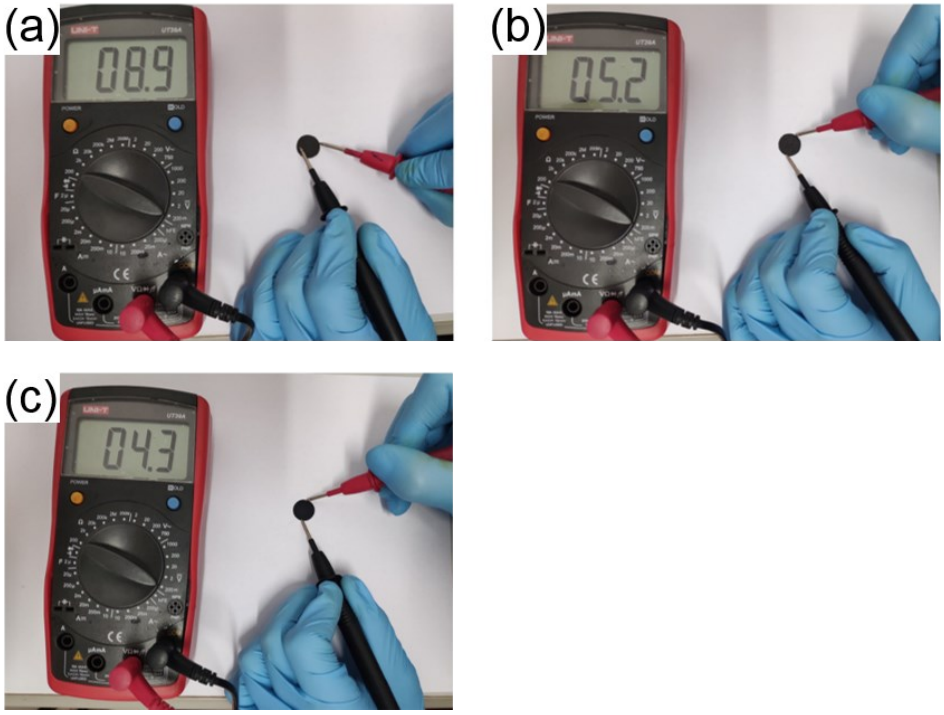

Fig. S3 Resistance measurement of CC (a), NPC@CC (b) and NPCM@CC (c) host with distance of 14 mm.

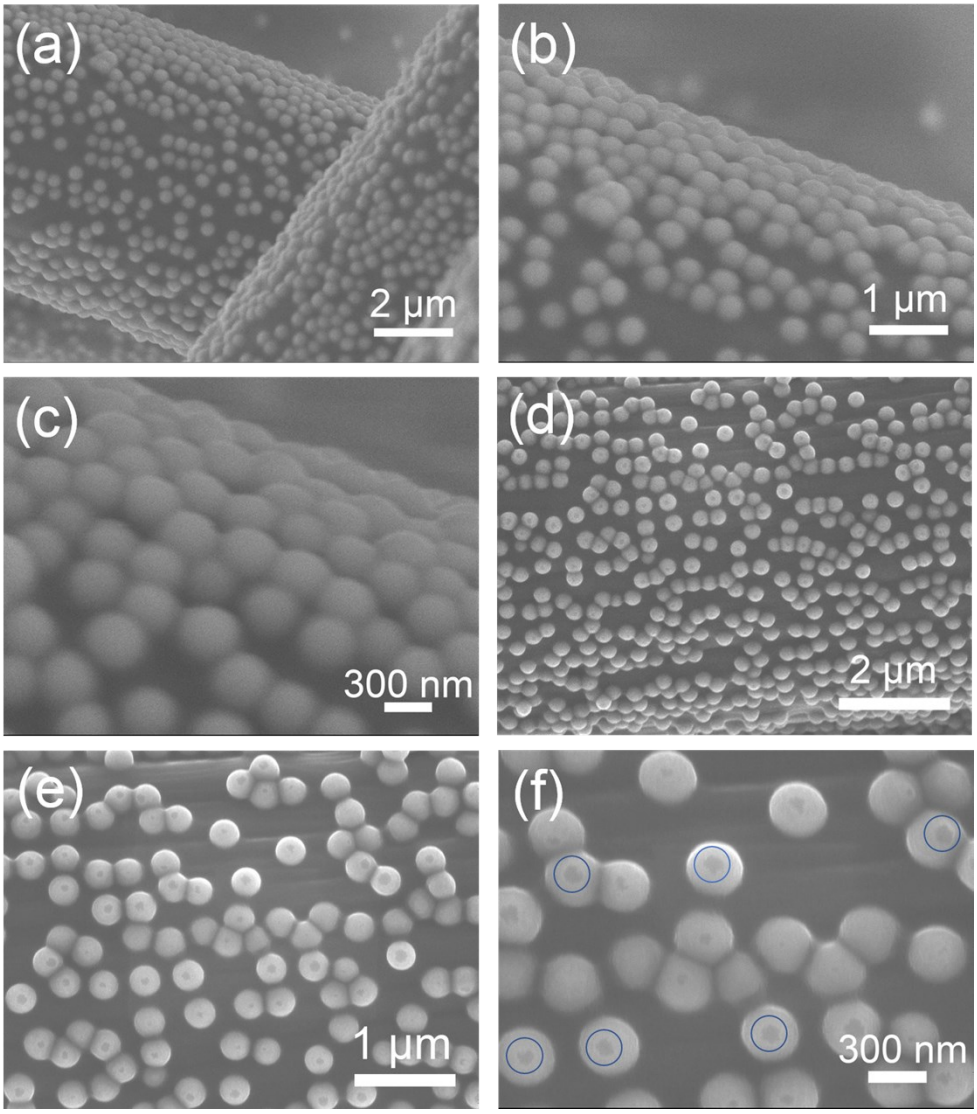

Fig.S4 SEM images of NPCM precursor gel@CC (a-c) and NPCM/SiO_2@CC (d-f). (b-c) and (e-f) are magnified SEM images. The blue circles in (f) indicate small cracks and holes at the top of carbon microcavities.

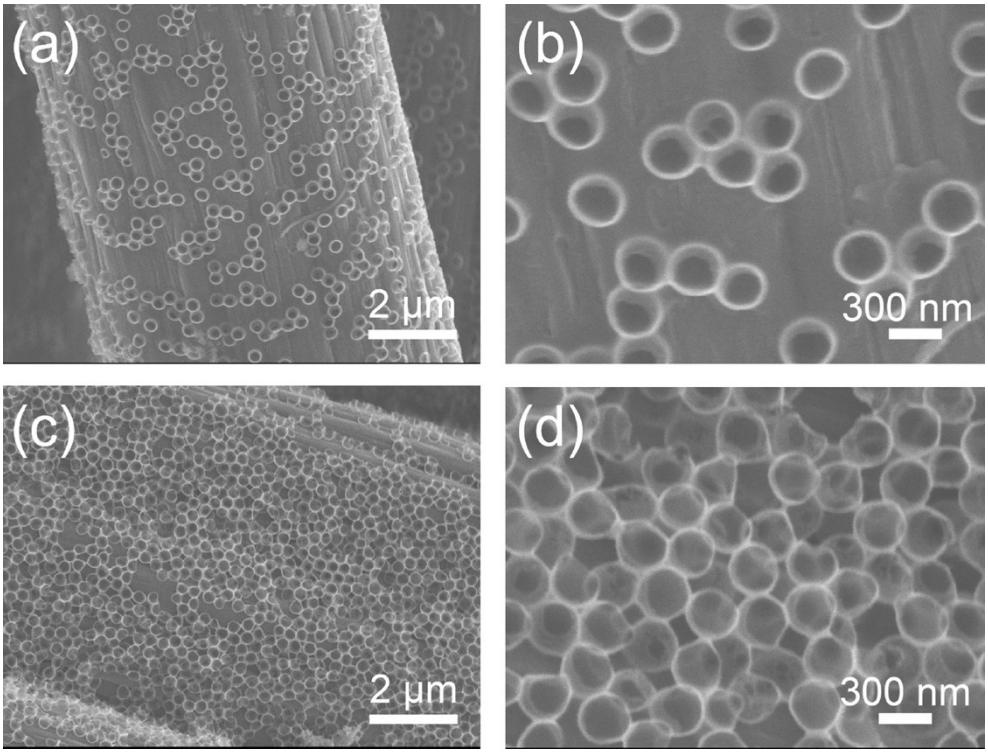

Fig.S5 SEM images of NPCM@CC-5 and NPCM@CC-20 prepared with 5 mg ml^{-1} (a, b) and 20 mg ml^{-1} (c, d) SiO_2 template, respectively. (b) and (d) are magnified SEM images.

Table S1 Basic properties of three different host materials.

Samples	BET specific surface area (m^2 g^{-1})	Pore volume (10^{-3} * cm^3 g^{-1})	N content (atom %)	I_G/I_D
CC	0.4	0.44	0	1.04
NPC@CC	11.8	7.3	3.30	1.06
NPCM@CC	10.8	6.7	4.01	1.10

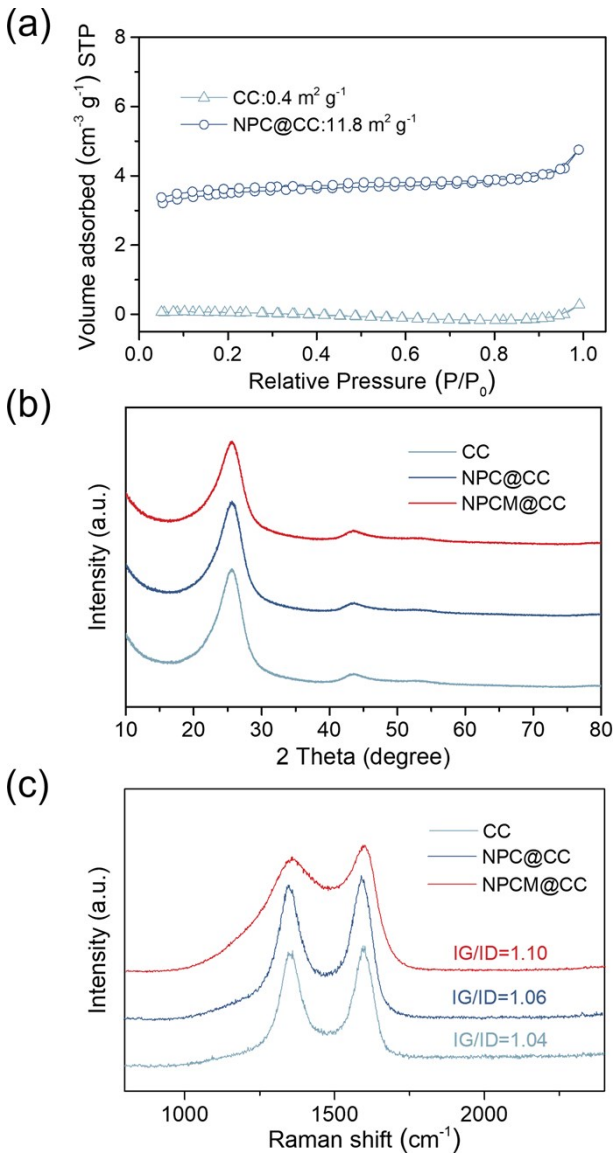

Fig. S6 (a) N_2 adsorption-desorption isotherms of CC and NPC@CC. XRD patterns (b) and Raman spectra (c) of CC, NPC@CC, and NPCM@CC.

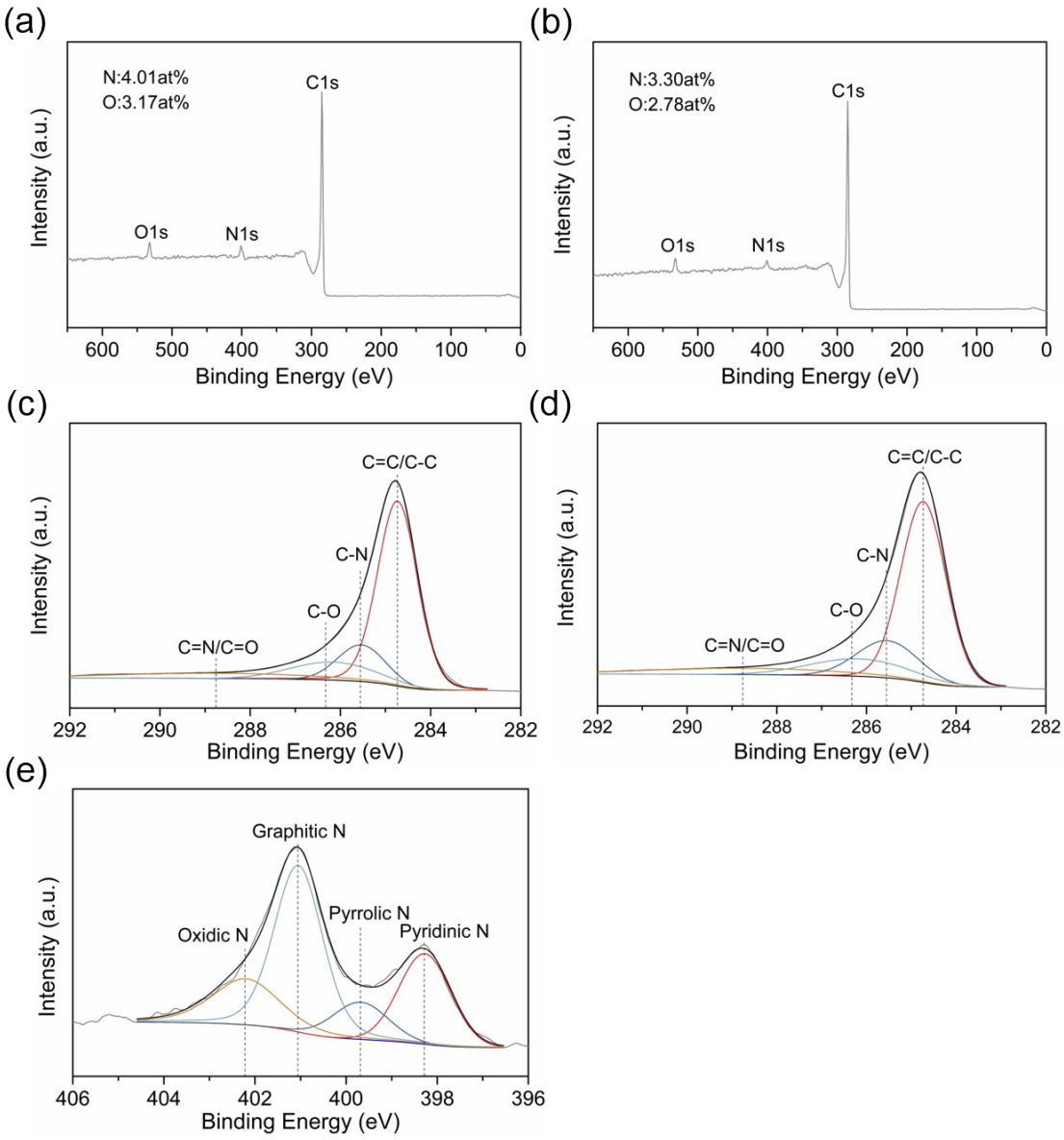

Fig. S7 XPS spectra of NPCM@CC (a) and NPC@CC (b). High-resolution C 1s spectrum of NPCM@CC (c) and NPC@CC (d). (e) High-resolution N 1s spectrum of NPC@CC

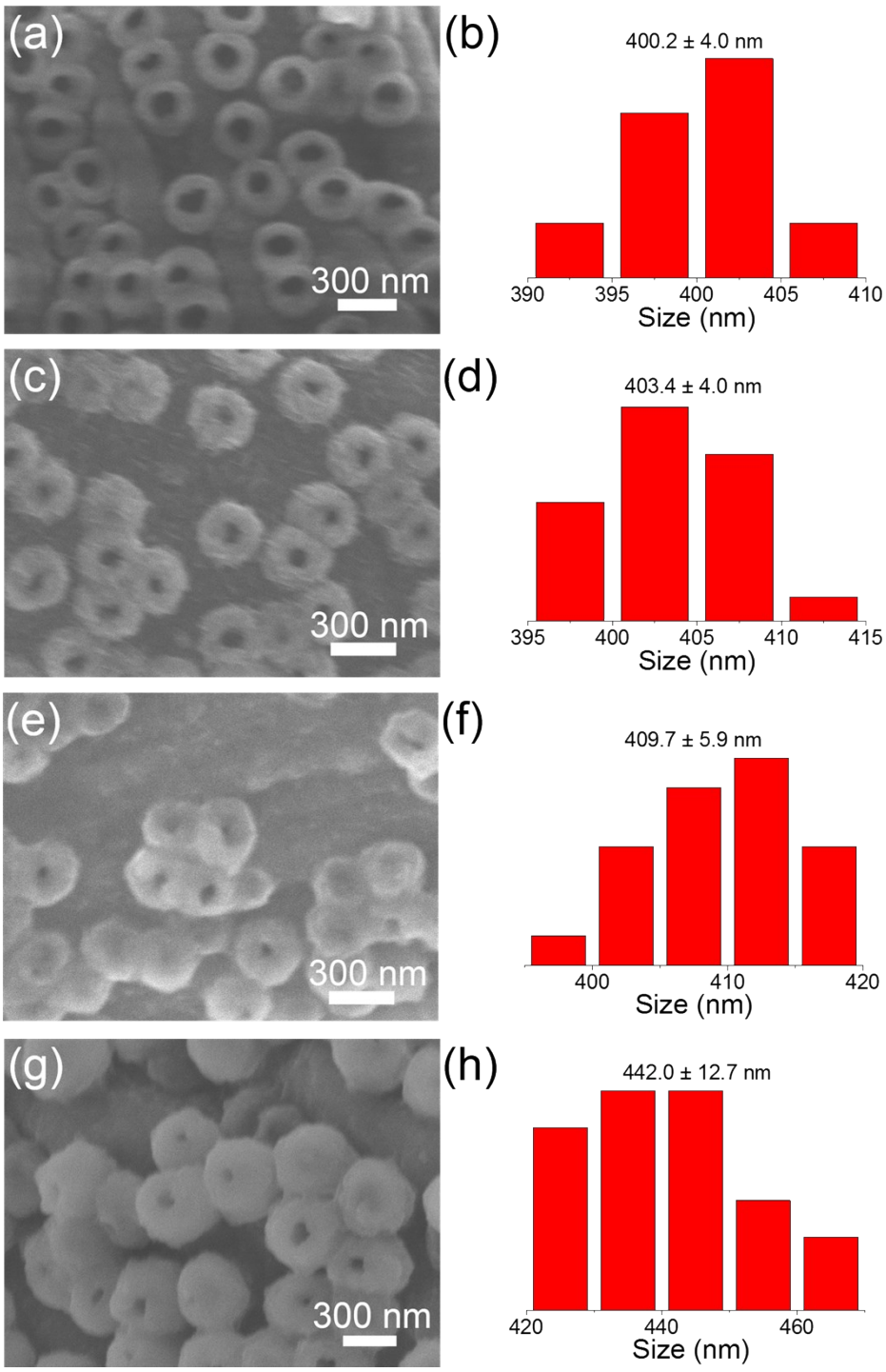

Fig. S8 High-resolution SEM images of NPCM@CC electrode and corresponding size distribution of carbon microcavities when it lithiated to 0 (a, b), 3 (c, d), 5 (e, f), and 8 mAh cm^{-2} (g, f), respectively.

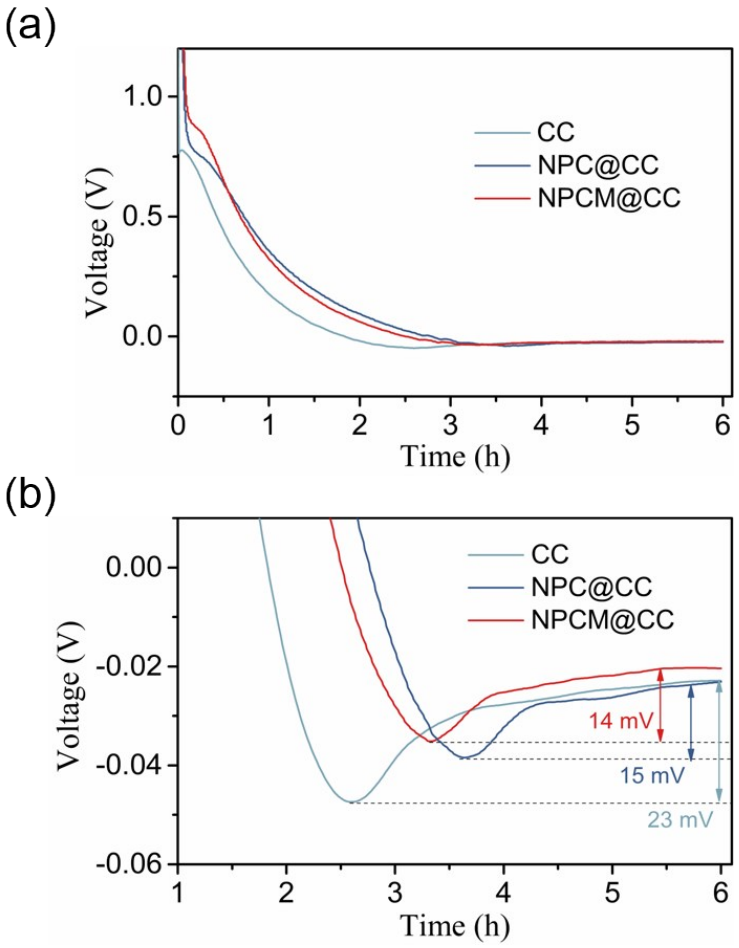

Fig. S9 The initial discharge curve (a) and its voltage dip in the range of -0.06-0.01 V (b) of CC, NPC@CC, and NPCM@CC.

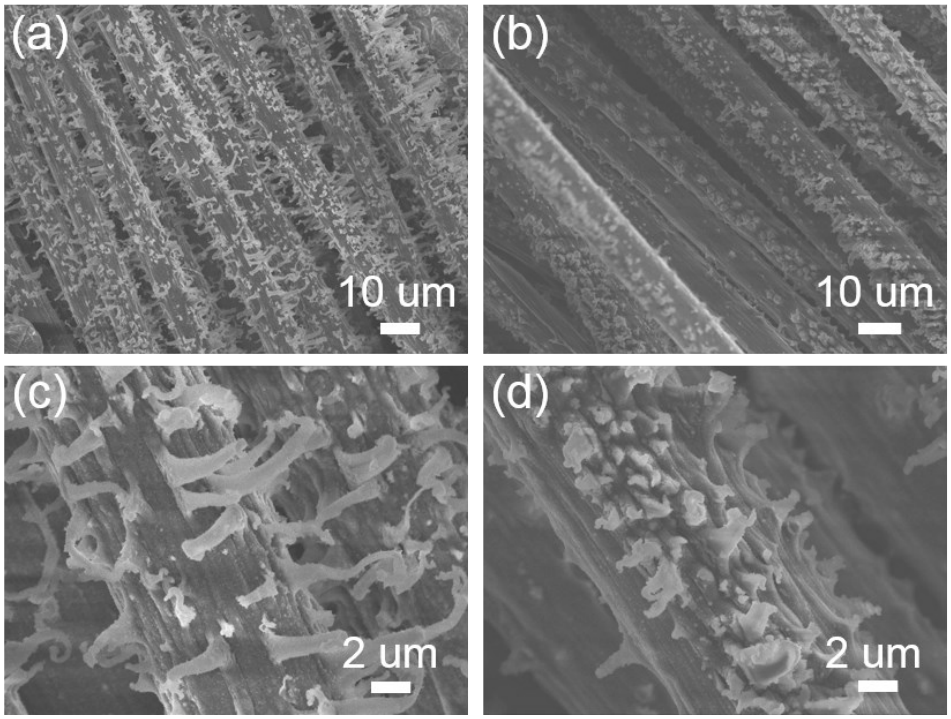

Fig. S10 SEM images of CC (a), (c) and NPC@CC (b), (d) after inserting/plating 5 mA h cm^{-2} Li. (c) and (d) are magnified SEM images.

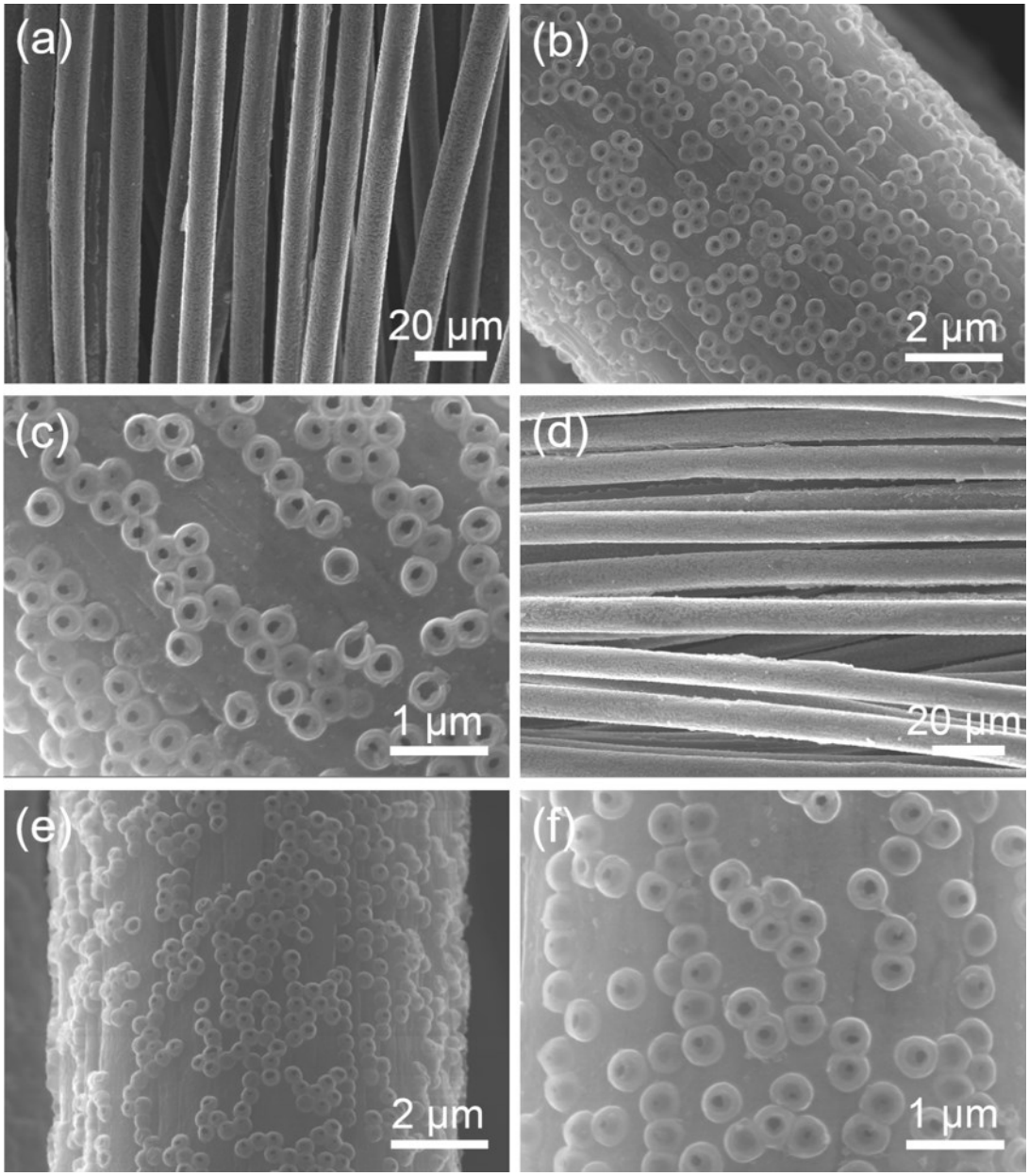

Fig. S11 SEM images of NPCM@CC after 50 (a-c) and 100 (d-f) cycles at 2 mA cm^{-2} and 1 mAh cm^{-2}. (b-c) and (e-f) are magnified SEM images of NPCM@CC.

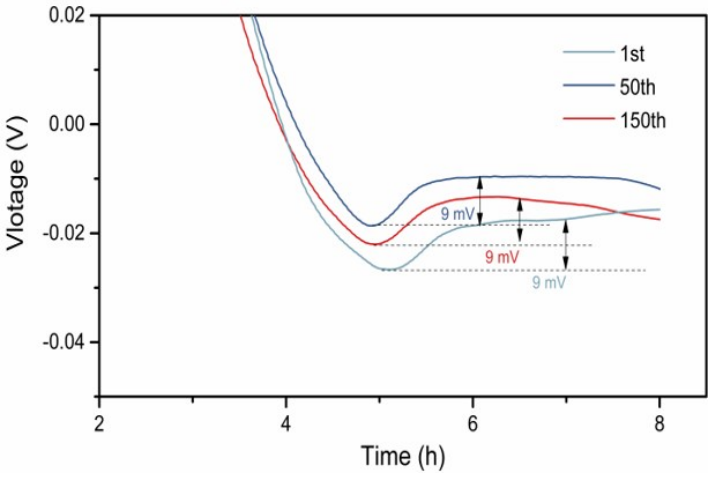

Fig. S12 The nucleation overpotential curves of NPCM@CC anode at 1, 50 and 150 cycles.

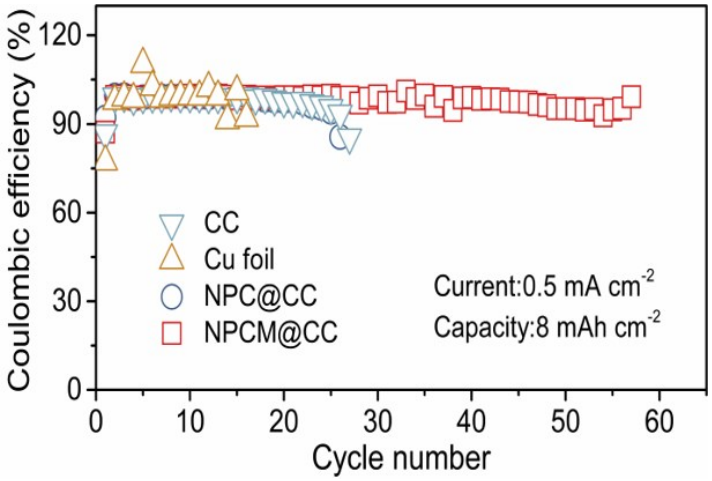

Fig. S13 Comparison of CE of the copper foil, pristine CC, NPC@CC and NPCM@CC electrodes with an areal capacity of 8.0 mA h cm^{-2} at a current density of 0.5 mA cm^{-2}.

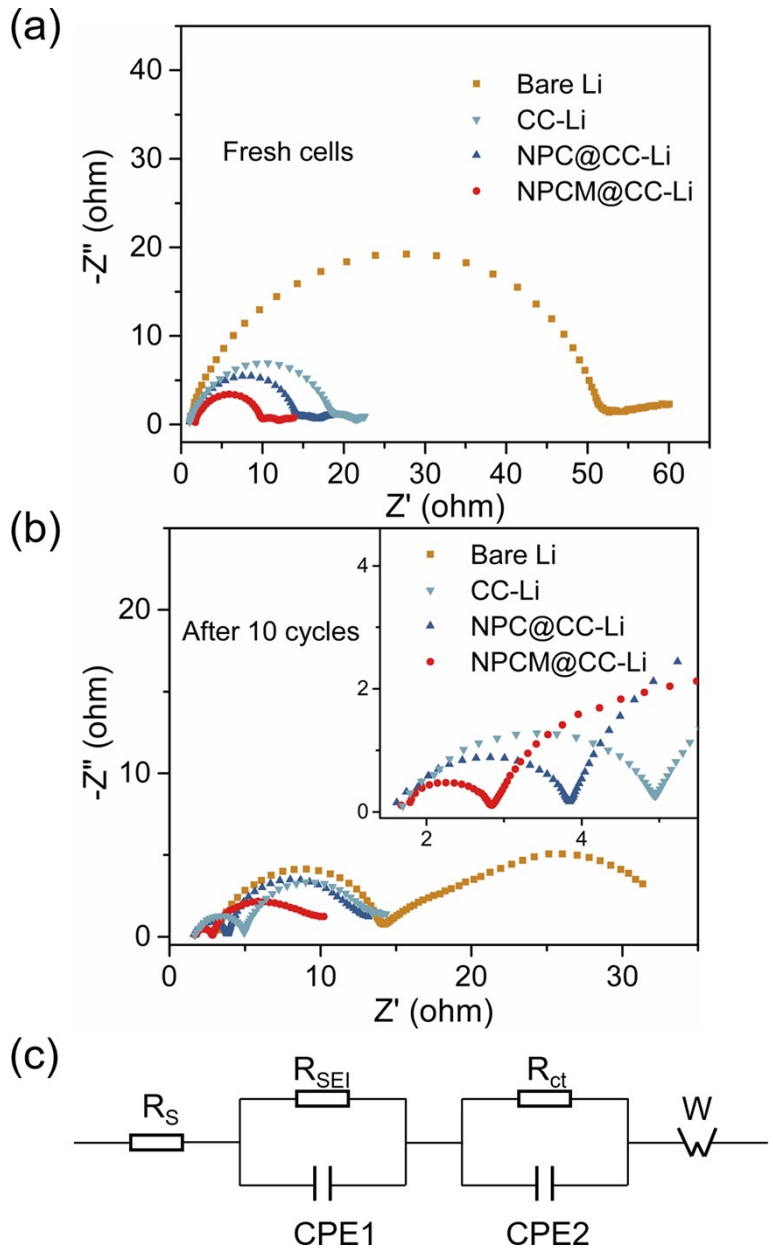

Fig. S14 The Nyquist plot of impedance curves for bare Li, CC-Li, NPC@CC-Li, and NPCM@CC-Li in symmetrical cells before (a) and after (b) 10 cycles with a current density of 1 mA cm^{-2} and areal capacity of 1 mAh cm^{-2}. (c) The equivalent circuit of these cells.

Table S2 Fitted EIS parameters

	Fresh cells			After 10 cycles		
	R_s (Ω)	R_{SEI} (Ω)	R_{ct} (Ω)	R_s (Ω)	R_{SEI} (Ω)	R_{ct} (Ω)
Bare Li	1.45	50.65	5.37	2.93	11.21	13.31
CC-Li	1.14	17.38	3.09	1.68	3.16	8.16
NPC@CC-Li	1.23	13.15	2.50	1.62	2.13	8.47
NPCM@CC-Li	1.79	7.96	2.36	1.75	1.08	5.63

Table S3 Comparison of the Coulombic efficiency of Li metal anodes with different carbon-based hosts.

hosts	Current (mA cm^{-2})	Capacity (mAh cm^{-2})	CE (%)	Cycle number	Ref.
rGO infiltrated Ni foam	0.5	1	95	100	1
	1	1	95	100	
Nitrogen-doped graphene	1	1	98	200	2
	1	2	98	50	
CNT sponge	1	2	98.5	90	3
Graphitized carbon fibers	0.5	8	98	50	4
CNTs Modified Carbon Cloth	1	1	99	100	5
N-doped carbon rod array	1	1	98	120	6
	1	2	97	80	
3D CNT host on Cu foil	1	1	99	250	7
	1	5	/	30	
3D fluoride graphene	2	1	98	150	8
	1	2	/	88	
NPCM@CC	0.5	4	99.1	150	This work
	0.5	8	98.1	57	
	1	4	99.0	90	

Table S4 Comparison of galvanostatic cycling performance of symmetric cells with different Carbon-based hosts for Li metal anodes.

hosts	Current (mA cm^{-2})	Capacity (mAh cm^{-2})	Overpotential (mV)	lifespan (h)	Ref.
rGO infiltrated Ni foam	0.2	0.8	/	100	1
Nitrogen-doped graphene	1	0.042	40	200	2
Graphitized carbon fibers	1	1	20	1000	4
	2	1	/	300	
N-doped carbon rod array	1	1	12	1350	6
	2	1	20	620	
3D CNT host on Cu foil	1	1	15	200	7
3D fluoride graphene	0.5	1	10	800	8
	1	2	50	350	
CNTs Modified Carbon Cloth	1	1	18	500	9
	2	1	23	500	
Carbon cloth-based lithium	1	1	46	400	10
NPCM@CC	1	1	9	4200	This work
	2	1	10	1200	

References

1 H. Yan, C. Shen, K. Yuan, K. Zhang, X. Liu, J.-G. Wang and K. Xie, *ACS Sustain. Chem. Eng.*, 2018, **6**, 4776-4783.

2 R. Zhang, X. R. Chen, X. Chen, X. B. Cheng, X. Q. Zhang, C. Yan and Q. Zhang, *Angew. Chem. Int. Ed.*, 2017, **56**, 7764-7768.

3 G. Yang, Y. Li, Y. Tong, J. Qiu, S. Liu, S. Zhang, Z. Guan, B. Xu, Z. Wang and L. Chen, *Nano Lett.*, 2019, **19**, 494-499.

4 T. T. Zuo, X. W. Wu, C. P. Yang, Y. X. Yin, H. Ye, N. W. Li and Y. G. Guo, *Adv. Mater.*, 2017, **29**, 1700389.

5 F. Liu, R. Xu, Z. Hu, S. Ye, S. Zeng, Y. Yao, S. Li and Y. Yu, *Small*, 2019, **15**, 1803734.

6 L. Chen, H. Chen, Z. Wang, X. Gong, X. Chen, M. Wang and S. Jiao, *Chem. Eng. J.*, 2019, **363**, 270-277.

7 F. Shen, F. Zhang, Y. Zheng, Z. Fan, Z. Li, Z. Sun, Y. Xuan, B. Zhao, Z. Lin, X. Gui, X. Han, Y. Cheng and C. Niu, *Energy Storage Mater.*, 2018, **13**, 323-328.

8 Z. Li, X. Li, L. Zhou, Z. Xiao, S. Zhou, X. Zhang, L. Li and L. Zhi, *Nano Energy*, 2018, **49**, 179-185.

9 F. Liu, R. Xu, Z. Hu, S. Ye, S. Zeng, Y. Yao, S. Li and Y. Yu, *Small*, 2019, **15**, 1803734.

10 Y. Zhou, Y. Han, H. Zhang, D. Sui, Z. Sun, P. Xiao, X. Wang, Y. Ma and Y. Chen, *Energy Storage Mater.*, 2018, **14**, 222-229.